Supplementary

The detail of histological findings, baseline chest imaging, and comprehensive pulmonary function test of each patient

No. 1

Histological findings:

A biopsy specimen of the upper and lower lobe of the left lung presented lymph follicle formation and infiltration of lymphoplasmacytic cells in the alveolar interstitium and bronchovascular bundle. A mediastinal lymph node sample presented plasmacytosis in the interfollicular space, and the infiltrated plasma cells did not present deviation of κ / λ ratio by light chain in situ hybridization (ISH).

Chest imaging at baseline:

Diffuse ground-glass opacity and interlobular septal thickening were found.

Pulmonary function test. (at baseline)	
VC (L)	3.97
VC % predicted (%)	87
FEV1.0 (L)	8.46
FEV1.0% (%)	89.9
DLco % predicted (%)	79.6

VC, Vital capacity; FEV, Forced expiratory volume in one second; DLco, diffusing capacity of lung for carbon monoxide.

https://dx.doi.org/10.21037/jtd-21-1973

No. 2

Histological findings:

A biopsy specimen of the middle and lower lobe of the right lung revealed infiltration of lymphocytes and plasma cells. Fibrotic interstitial change and developing germinal center were partly shown. $IgG4^+/IgG^+$ ratio was not too high, although dying was weak.

Chest imaging at baseline:

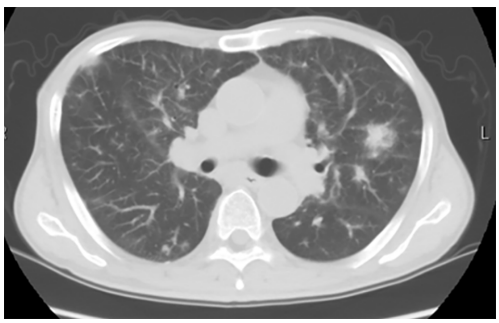

Patchy shadow and diffuse ground-glass opacity were shown.

Pulmonary function test. (at baseline)	
VC (L)	2.55
VC % predicted (%)	74.5
FEV1.0 (L)	2.08
FEV1.0% (%)	76.4
DLco % predicted (%)	77.2

https://dx.doi.org/10.21037/jtd-21-1973

No. 3

Histological findings:

A mediastinal lymph node biopsy specimen revealed plasmacytosis in the interfollicular space. $IgG4^+/IgG^+$ ratio was approximately 20%.

Chest imaging at baseline:

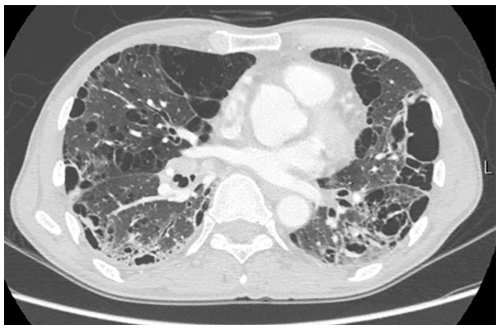

Multiple cystic changes and reticular and ground-glass opacities were shown in the predominantly bilateral lower lobes of the lungs.

Pulmonary function test. (at baseline)

VC (L)	2.76
VC % predicted (%)	65.4
FEV1.0 (L)	1.90
FEV1.0% (%)	69.6
DLco % predicted (%)	34.2

https://dx.doi.org/10.21037/jtd-21-1973

No. 4

Histological findings:

A biopsy specimen of the upper and lower lobe of the right lung revealed aggregation of small lymphoid cells around the bronchiole. The infiltration of plasma cells was shown. $IgG4^{+}/IgG^{+}$ ratio was approximately 10%.

Chest imaging at baseline:

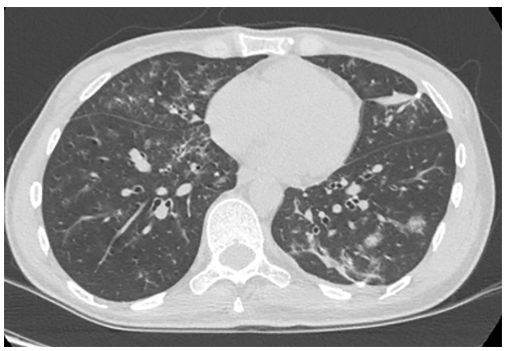

Diffuse ground-glass opacities were shown.

Pulmonary function test. (at baseline)	
VC (L)	2.54
VC % predicted (%)	79.1
FEV1.0 (L)	1.56
FEV1.0% (%)	64.5
DLco % predicted (%)	77.7

https://dx.doi.org/10.21037/jtd-21-1973

No. 5

Histological findings:

A biopsy specimen of the upper and lower lobe of the left lung revealed the infiltration of plasma cells in the alveolar interstitium. $IgG4^+/IgG^+$ ratio was approximately 20% and 50% in lung and mediastinal lymph node specimens, respectively.

Chest imaging at baseline:

Diffuse ground-glass opacities and thickened bronchovascular bundles were shown.

Pulmonary function test. (at baseline)	
VC (L)	3.61
VC % predicted (%)	89.5
FEV1.0 (L)	2.75
FEV1.0% (%)	76.8
DLco % predicted (%)	91.4

https://dx.doi.org/10.21037/jtd-21-1973

Table S1 Changes of imaging findings of the lung and symptoms before and after treatment

Patient No	Change of image findings of lung	Change of symptom
No. 1	Multi cystic change appeared. Ground grass opacity improved.	Fever and dyspnea on exertion improved.
No. 2	Ground glass opacity partially improved and partially progressed.	No symptom at first visit and no change.
No. 3	Multi cystic change progressed.	Dyspnea on exertion and cough were not changed.
No. 4	Ground glass opacity partially improved.	Fever and fatigue improved.
No. 5	Ground glass opacity were not changed.	Dyspnea on exertion was not changed.

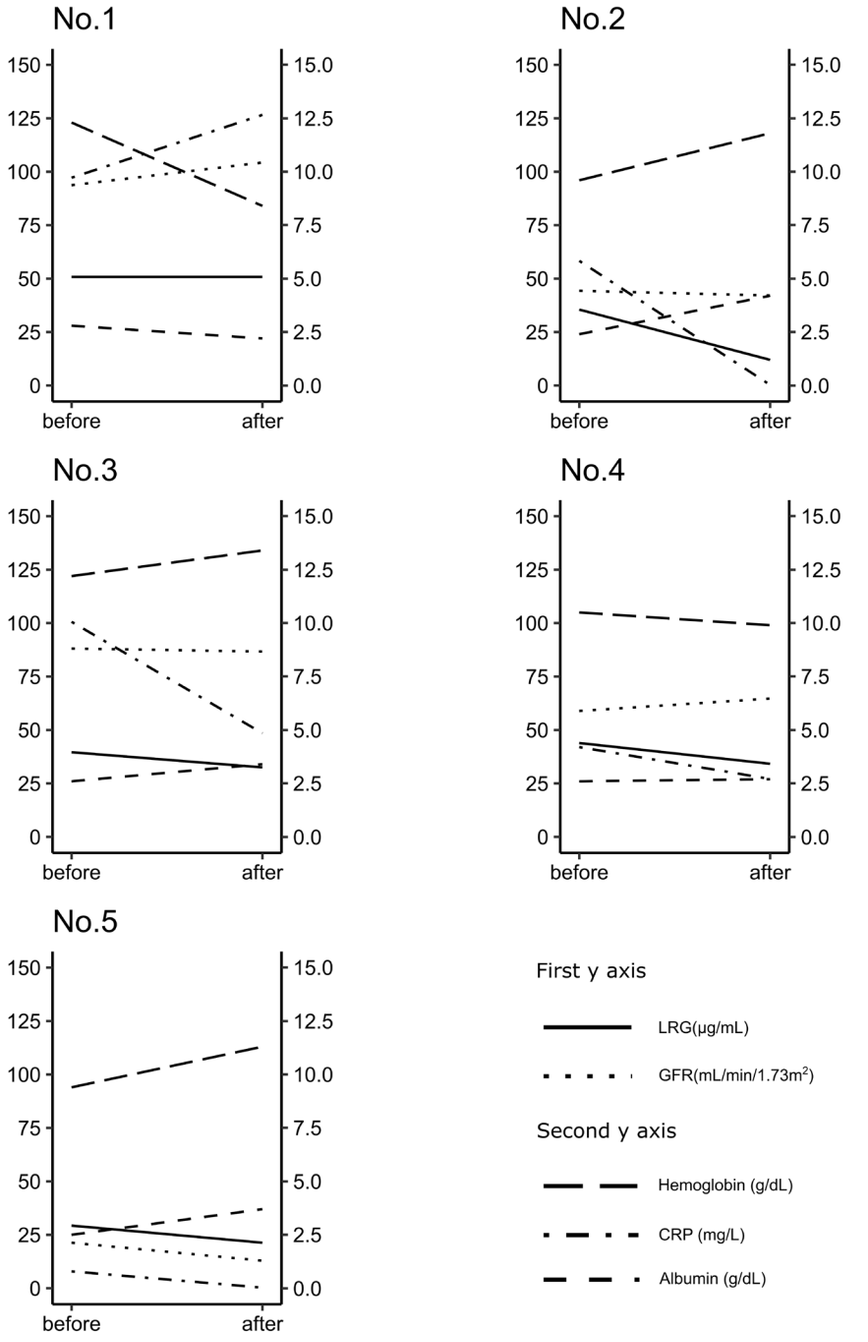

Figure S1 Biochemical findings before and after treatment. LRG tended to correlate with biochemical values such as hemoglobin, albumin, and CRP.

https://dx.doi.org/10.21037/jtd-21-1973

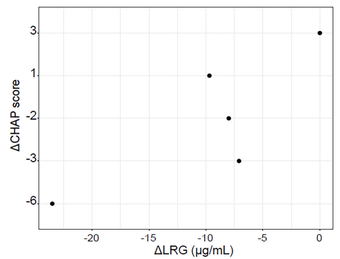

Figure S2 Correlation of ΔLRG and ΔCHAP score. The ΔLRG tended to correlate with ΔCHAP score, although not statistically significant due to the small sample size. (Polyserial correlation coefficient = 0.8795, P value =0.7818).

Table S2 Cytokine and chemokine quantification

	CXCL1	CXCL9	CXCL11	IL-10	MIP-1α	ENA-78	MIP-1β	MIP-3α	Eotaxin	IL-8	CXCL10	MCP-1	TARC	APRIL	BAFF	IL-6	IL-17A	IFN-γ	IL-2	IL-4	IL-12p70	IL-13	sCD40L	TNF-α	TNF-β
MCD	193.2	142	60.3	15.5	343.1	423.5	35.3	38.5	153.6	219.5	64.4	316.6	251.3	13401.5	2849.6	67.2	19.1	2.5	68.3	38.8	49	10.9	10556.3	66.4	52.7
(n=5)	(182.3–255)	(70–380.6)	(32.3–2305)	(2–24.3)	(153.6–536.6)	(202.8–542.8)	(21–83.8)	(19.3–86.1)	(65.4–12000)	(94.3–1409.4)	(55.3–178)	(166.6–1542.3)	(115–287.3)	(12353.6–15520.3)	(1562.2–3812.5)	(47.7–633)	(3.6–34.9)	(2.5–26.1)	(22.5–249.9)	(6.4–77.9)	(45.1–56.3)	(4.8–43.9)	(3499.3–16400.3)	(3.4–235.4)	(21.9–319.9)
Control	96.6	64.6	18.9	2	112.5	227.3	86.5	35.9	75.2	1035	93.8	229.6	196.6	11681.1	1838.8	25.6	3.6	2.5	22.5	10.5	35.7	13.4	12959.4	16.7	106.9
(n=3)	(83.8–155.9)	(55.2–64.7)	(15.6–19.6)	(2–4.1)	(60.5–287.7)	(178.2–355.1)	(18.5–115.7)	(33.9–47.8)	(25.4–85.5)	(174.9–1109.6)	(91–94.3)	(189.6–379.3)	(147.7–536.5)	(10101.9–11765.2)	(1552.1–2878.6)	(4.5–88.2)	(3.6–14.9)	(2.5–15.9)	(22.5–22.5)	(3.6–34.1)	(26.1–60)	(4.8–20.6)	(9708–17445.1)	(15.8–78.4)	(95.4–315.4)
p-value (permutation test)	0.03571	0.03571	0.03571	0.1429	0.07143	0.25	0.5714	0.5714	0.3929	1	0.7857	1	0.7857	0.03571	0.3929	0.25	0.2321	0.6429	0.2857	0.1429	0.5714	0.7857	0.5714	0.5714	0.5714

MCD, multicentric Castleman disease; IL, interleukin; MIP, macrophage inflammatory protein; MCP, monocyte chemoattractant protein; APRIL, a proliferation-inducing ligand; IFN, interferon; TNF, tumor necrosis factor

https://dx.doi.org/10.21037/jtd-21-1973